AD-A167 340 A NEW EFFICIENT APPROACH TO THE FORMULATION OF MIXED FINITE ELEMENT MODEL..(U) MARYLAND UNIV COLLEGE PARK DEPT OF AEROSPACE ENGINEERING S W LEE ET AL. FEB 86 1/1

UNCLASSIFIED N00014-84-K-0385 F/G 20/11 NL

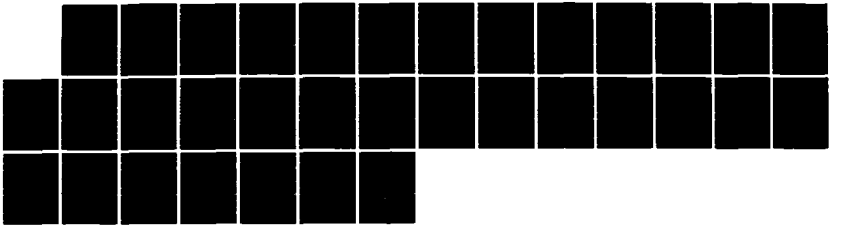

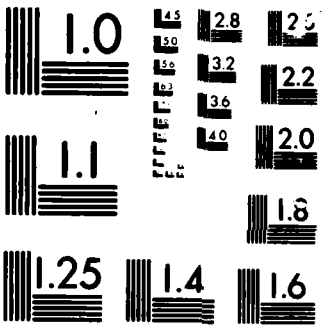

MICROCOPY CHART

(12)

A NEW EFFICIENT APPROACH TO THE FORMULATION OF MIXED FINITE ELEMENT MODELS FOR STRUCTURAL ANALYSIS

S.W. LEE

J.J. RHIU

February 1986

INTERIM REPORT

Office of Naval Research
Contract No. N00014-84-K-0385
Work Unit No. NR064-718/4-6-84(432S)

unclassified
SECURITY CLASSIFICATION OF THIS PAGE

ADA167340

REPORT DOCUMENTATION PAGE

1a. REPORT SECURITY CLASSIFICATION: Unclassified	1b. RESTRICTIVE MARKINGS
2a. SECURITY CLASSIFICATION AUTHORITY	3. DISTRIBUTION/AVAILABILITY OF REPORT: Unlimited
2b. DECLASSIFICATION/DOWNGRADING SCHEDULE	
4. PERFORMING ORGANIZATION REPORT NUMBER(S)	5. MONITORING ORGANIZATION REPORT NUMBER(S)
6a. NAME OF PERFORMING ORGANIZATION: Department of Aerospace Eng. University of Maryland; 6b. OFFICE SYMBOL (If applicable)	7a. NAME OF MONITORING ORGANIZATION: Office of Naval Research Mechanics Division
6c. ADDRESS (City, State and ZIP Code): College Park, Maryland 20742	7b. ADDRESS (City, State and ZIP Code): 800 North Quincy Street Arlington, VA 22217
8a. NAME OF FUNDING/SPONSORING ORGANIZATION: Office of Naval Research; 8b. OFFICE SYMBOL (If applicable)	9. PROCUREMENT INSTRUMENT IDENTIFICATION NUMBER: N00014-84-K-0385
8c. ADDRESS (City, State and ZIP Code): 800 North Quincy Street Arlington, VA 22217	10. SOURCE OF FUNDING NOS.

PROGRAM ELEMENT NO.	PROJECT NO.	TASK NO.	WORK UNIT NO.
			NR064-718/ 4-6-84(432 S)

11. TITLE (Include Security Classification) A New Efficient Approach to the Formulation of Mixed Finite Element Models for Structural Analysis

12. PERSONAL AUTHOR(S): S.W. Lee and J.J. Rhiu

13a. TYPE OF REPORT	13b. TIME COVERED	14. DATE OF REPORT (Yr., Mo., Day)	15. PAGE COUNT
interim	FROM May 1986 TO June 1986	Feb 1986	30

16. SUPPLEMENTARY NOTATION

17. COSATI CODES			18. SUBJECT TERMS (Continue on reverse if necessary and identify by block number)
FIELD	GROUP	SUB. GR.	new mixed formulation, Hellinger-Reissner principle, lower order and higher order assumed strain

19. ABSTRACT (Continue on reverse if necessary and identify by block number)

A new finite element formulation is developed based on the Hellinger-Reissner principle with independent strain. By dividing the assumed strain into the lower order part and the higher order part, the new formulation can be made much more efficient than the standard mixed formulation. In addition the present new approach provides a rational way of introducing stabilization matrix to suppress undesirable kinematic modes.

20. DISTRIBUTION/AVAILABILITY OF ABSTRACT	21. ABSTRACT SECURITY CLASSIFICATION
UNCLASSIFIED/UNLIMITED ☐ SAME AS RPT. ☐ DTIC USERS ☐	unclassified

22a. NAME OF RESPONSIBLE INDIVIDUAL	22b. TELEPHONE NUMBER (Include Area Code)	22c. OFFICE SYMBOL
Dr. R.E. Whitehead, Mechanics Division, ONR	(202)-696-4305	

FORM 1473, 83 APR EDITION OF 1 JAN 73 IS OBSOLETE.

unclassified
SECURITY CLASSIFICATION OF THIS PAGE

A NEW EFFICIENT APPROACH TO THE FORMULATION OF MIXED FINITE ELEMENT MODELS FOR STRUCTURAL ANALYSIS

S.W. LEE

J.J. RHIU

February 1986

INTERIM REPORT

Office of Naval Research
Contract No. N00014-84-K-0385
Work Unit No. NR064-718/4-6-84(432S)

SUMMARY

A new mixed finite element formulation is developed based on the Hellinger-Reissner principle with independent strain. By dividing the assumed strain into the lower order part and the higher order part, the new formulation can be made much more efficient than the standard mixed formulation. In addition the present new approach provides an alternative way of introducing stabilization matrix to suppress undesirable kinematic modes.

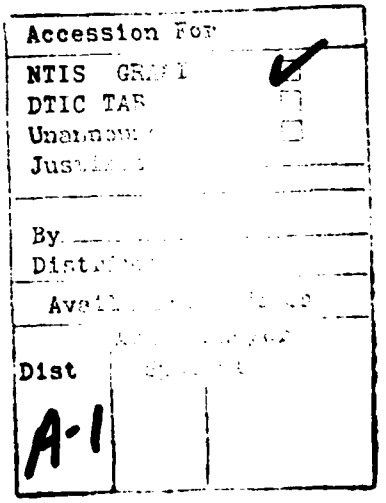

1. INTRODUCTION

Hybrid and mixed finite element formulations based on the Hellinger-Reissner principle or related variational principles have been available since the early days in the history of finite element method [1]. In these formulations an independent stress or strain is assumed within an element in addition to the usual assumed displacement expressed in terms of nodal displacement. The independent stress or strain is eliminated at element level, resulting in an element stiffness matrix corresponding to nodal displacement vector. Note that in this paper we are not interested in the type of mixed formulation used in reference 9 where both nodal displacements and nodal stress variables remain in the assembled global model. For an element with a given number of nodes there is a degree of flexibility in the choice of assumed stress or strain. For example in the case of Pian's original assumed stress hybrid model [2], the assumed stress is chosen to satisfy equilibrium within an element. Of course, the property of the stiffness matrix depends very much on the assumed stress or strain. Thus with a proper choice of assumed stress or strain it is possible to develop a finite element model which is superior to the conventional finite element model based purely on the assumed displacement approach. For example, for thin plates and shells, a mixed formulation based on the Hellinger-Reissner principle or the modified Hellinger-Reissner principle can be used to alleviate the undesirable locking effect associated with the condition of zero inplane strain and zero transverse shear strain imposed on a finite element model [3,4]. The role of hybrid and mixed formulations in conjunction with nearly incompressible materials has also been studied [5]. Moreover a mixed formulation provides a rational mathematical basis for the popular reduced and selective integration scheme [6-8].

However, in hybrid and mixed formulations it is necessary to invert a

matrix in order to generate an element stiffness matrix. Therefore, in comparison with the assumed displacement model based on the principle of virtual work, hybrid and mixed formulations require usually more time to compute element stiffness matrix of the same size. This fact has been regarded as the major drawback of the conventional hybrid and mixed formulations.

With this in mind, we present in this paper a new mixed formulation which requires much less computing time than the conventional mixed formulation for the generation of element stiffness matrix. The new formulation is based on the Hellinger-Reissner principle with independent strain. The new formulation can be applied to any type of problems in solid and structural mechanics. However, for simplicity, two dimensional plane problems will be used to demonstrate the effectiveness of the approach. Initially nine node element will be used for the purpose of illustration. A short discussion on four node element will follow. In order to contrast the new formulation with the conventional formulation, we will start off with the conventional formulation.

2. CONVENTIONAL MIXED FORMULATION

2.1 Finite Element Formulation

For two dimensional plane problem, the functional π_R for the Hellinger-Reissner principle can be written as

$$\pi_R = \int_A (\underset{\sim}{\varepsilon}^T \underset{\sim}{C} \bar{\underset{\sim}{\varepsilon}} - \frac{1}{2}\underset{\sim}{\varepsilon}^T \underset{\sim}{C} \underset{\sim}{\varepsilon})\, dA - W \qquad (1)$$

where

$$\underset{\sim}{\varepsilon} = \begin{Bmatrix} \varepsilon_{xx} \\ \varepsilon_{yy} \\ \varepsilon_{xy} \end{Bmatrix} \quad : \text{ independent strain vector}$$

$$\bar{\underset{\sim}{\varepsilon}} = \begin{Bmatrix} \bar{\varepsilon}_{xx} \\ \bar{\varepsilon}_{yy} \\ \bar{\varepsilon}_{xy} \end{Bmatrix} = \begin{Bmatrix} \frac{\partial u}{\partial x} \\ \frac{\partial v}{\partial y} \\ \frac{\partial u}{\partial y} + \frac{\partial v}{\partial x} \end{Bmatrix}$$: strain vector in terms of displacement field

u, v: displacement in x and y direction respectively

A: area

W: external load term

$\underset{\sim}{C}$: 3 x 3 matrix of elastic constants integrated through thickness

Note that in eg. (1) instead of stress, strain $\underset{\sim}{\varepsilon}$ appears as independent variables in addition to displacement field u and v.

For finite element approximation, the displacement vector $\underset{\sim}{u}$ is assumed in terms of nodal displacement vector as

$$\underset{\sim}{u} = \begin{Bmatrix} u \\ v \end{Bmatrix} = \underset{\sim}{N}\, q_e \tag{2}$$

where $\underset{\sim}{N}$: shape function matrix

q_e: element nodal displacement vector

Then the strain vector $\bar{\underset{\sim}{\varepsilon}}$ can be written symbolically as

$$\bar{\underset{\sim}{\varepsilon}} = \underset{\sim}{B}\, q_e \tag{3}$$

where $\underset{\sim}{B}$ is the matrix relating $\bar{\underset{\sim}{\varepsilon}}$ to q_e.

In addition, within each element the independent strain $\underset{\sim}{\varepsilon}$ is assumed in terms of unknown coefficients as

$$\underset{\sim}{\varepsilon} = \underset{\sim}{P}\underset{\sim}{\alpha} \tag{4}$$

where $\underset{\sim}{P}$: strain shape function matrices

$\underset{\sim}{\alpha}$: vector of unknown coefficients in an element

Introducing eq. (3) and (4) into eq. (1).

$$\pi_R = \sum(\underset{\sim}{\alpha}^T \underset{\sim}{G}\, \underset{\sim}{q}_e - \frac{1}{2}\underset{\sim}{\alpha}^T \underset{\sim}{H}\underset{\sim}{\alpha} - \underset{\sim}{q}_e^T \underset{\sim}{Q}_e) \tag{5}$$

with

$$\underset{\sim}{G} = \int_{A_e} \underset{\sim}{P}^T \underset{\sim}{C}\, \underset{\sim}{B}\, dA \tag{5a}$$

$$\underset{\sim}{H} = \int_{A_e} \underset{\sim}{P}^T \underset{\sim}{C}\, \underset{\sim}{P}\, dA \tag{5b}$$

$$W = \sum \underset{\sim}{q}_e^T \underset{\sim}{Q}_e \tag{5c}$$

and A_e is the element area.

The summation sign indicates summation or assembly over all elements.

Taking $\delta\pi_R = 0$ with respect $\underset{\sim}{\alpha}$ in each element,

$$\underset{\sim}{G}\, \underset{\sim}{q}_e - \underset{\sim}{H}\, \underset{\sim}{\alpha} = 0 \tag{6}$$

or solving for $\underset{\sim}{\alpha}$

$$\underset{\sim}{\alpha} = \underset{\sim}{H}^{-1} \underset{\sim}{G}\, \underset{\sim}{q}_e \tag{7}$$

for each element.

Substituting eq. (7) into eq. (5), π_R is written as

$$\pi_R = \sum_e \left(\frac{1}{2} q_e^T \underset{\sim}{K}_e q_e - q_e^T Q_e\right) \tag{8}$$

where $$\underset{\sim}{K}_e = \underset{\sim}{G}^T \underset{\sim}{H}^{-1} \underset{\sim}{G} \tag{9}$$

is the element stiffness matrix.

Assembling over all elements,

$$\pi_R = \frac{1}{2} q^T \underset{\sim}{K} q - q^T Q \tag{10}$$

where $\underset{\sim}{K}$: global stiffness matrix

q: global nodal displacement vector

Q: global load vector

Setting $\delta\pi_R = 0$ with respect to q leads to

$$\underset{\sim}{K} q = Q \tag{11}$$

which can be solved for q. With q thus q_e known, the independent strain vector ε in an element is determined by substituting eq. (7) to eq. (9) such that

$$\underset{\sim}{\varepsilon} = \underset{\sim}{P} \underset{\sim}{H}^{-1} \underset{\sim}{G} q_e \tag{12}$$

and, for isotropic materials, stress σ is determined as follows:

$$\underset{\sim}{\sigma} = \frac{1}{t} \underset{\sim}{C} \underset{\sim}{\varepsilon} \tag{13}$$

where t is the thickness.

2.2 Nine Node Element

The present nine node element is important in that it constitutes inplane part of the nine node shell element described in reference 4. This particular shell element has been found to be free of locking and any compatible or commutable kinematic mode. Of course a good nine node element is useful for plane stress and plane strain analysis itself. For the assumed displacement, the element shown in fig. 1 adopts the isoparametric representation. As for the coordinate system, global and local cartesian coordinate systems are used. The strains $\underset{\sim}{\varepsilon}$, $\bar{\underset{\sim}{\varepsilon}}$ and displacement u,v in eq. (1) are defined with respect to the global coordinate system. Local coordinate system is introduced to allow an assumed strain field with nonsymmetric polynomial terms. Local coordinate system is defined first by determining two unit vectors $\underset{\sim}{v}_1$ and $\underset{\sim}{v}_2$ at $\xi = \eta = 0$ point such that

$$\underset{\sim}{v}_1 = \frac{\partial \underset{\sim}{x}}{\partial \xi} \Big/ \left| \frac{\partial \underset{\sim}{x}}{\partial \xi} \right|$$

$$\underset{\sim}{v}_2 = \frac{\partial \underset{\sim}{x}}{\partial \eta} \Big/ \left| \frac{\partial \underset{\sim}{x}}{\partial \eta} \right| \qquad (14)$$

where $\underset{\sim}{x}$ is the position vector with components in the global coordinate system. The angle θ_o between these two unit vectors is calculated from the following equation:

$$\cos\theta_o = \underset{\sim}{v}_1 \cdot \underset{\sim}{v}_2 \qquad (15)$$

Then, if θ_o is less than or equal to 90^o, unit vector $\underset{\sim}{a}_1$ in the x direction of local coordinate system is defined as

$$\underset{\sim}{a}_1 = \frac{\partial \underset{\sim}{x}}{\partial \xi} \Big/ \left| \frac{\partial \underset{\sim}{x}}{\partial \xi} \right| \tag{16}$$

Otherwise $\underset{\sim}{a}_1$ is defined as

$$\underset{\sim}{a}_1 = \frac{\partial \underset{\sim}{x}}{\partial \eta} \Big/ \left| \frac{\partial \underset{\sim}{x}}{\partial \eta} \right| \tag{17}$$

Unit vector $\underset{\sim}{a}_2$ in the y direction of local coordinate system is orthogonal to $\underset{\sim}{a}_1$. Note that, while $\underset{\sim}{v}_1$ and $\underset{\sim}{v}_2$ are determined at $\xi = \eta = 0$ point, $\underset{\sim}{a}_1$ and $\underset{\sim}{a}_2$ can be computed at any point in the element. Especially $\underset{\sim}{a}_1$ and $\underset{\sim}{a}_2$ are needed at integration points to establish a local orthogonal coordinate system. Now, for the present nine node element, we may assume the independent strain in local coordinate system as follows;

$$\begin{aligned} \varepsilon^*_{xx} &= \alpha_1 + \alpha_2\xi + \alpha_3\eta + \alpha_4\xi\eta + \alpha_{13}f_x \\ \varepsilon^*_{yy} &= \alpha_5 + \alpha_6\xi + \alpha_7\eta + \alpha_8\xi\eta + \alpha_{14}f_y \\ \varepsilon^*_{xy} &= \alpha_9 + \alpha_{10}\xi + \alpha_{11}\eta + \alpha_{12}\xi\eta \end{aligned} \tag{18}$$

In eq. (18), $f_x = \xi\eta^2$ and $f_y = \xi^2\eta$ for $\underset{\sim}{a}_1$ defined as in eq. (16). For $\underset{\sim}{a}_1$ defined as in eq. (17), f_x and f_y are chosen as $f_x = \xi^2\eta$ and $f_y = \xi\eta^2$. Note that, due to the α_{13} and α_{14} terms, the assumed strains are not symmetric in ξ and η. However with the use of local coordinate system as defined here, the resulting stiffness matrix will not be dependent upon the choice of global coordinate system. Symbolically eq. (18) can be written as

$$\underset{\sim}{\varepsilon}^* = \underset{\sim}{P}^* \underset{\sim}{\alpha} \tag{19}$$

where $$\underset{\sim}{\varepsilon}^* = \begin{Bmatrix} \varepsilon^*_{xx} \\ \varepsilon^*_{yy} \\ \varepsilon^*_{xy} \end{Bmatrix} \tag{19a}$$

and $$\underset{\sim}{\alpha}^T = \lfloor \alpha_1 \; \alpha_2 \; \cdots \; \alpha_{14} \rfloor \tag{19b}$$

is the column vector of unknown strain coefficients, and $\underset{\sim}{P}^*$ is the 3 x 14 matrix containing polynomial terms in ξ and η coordinates. The strain vector $\underset{\sim}{\varepsilon}$ in global coordinate system is obtained from $\underset{\sim}{\varepsilon}^*$ through strain transformation matrix $\underset{\sim}{T}$ as follows:

$$\underset{\sim}{\varepsilon} = \underset{\sim}{T}\,\underset{\sim}{\varepsilon}^* = \underset{\sim}{T}\,\underset{\sim}{P}^*\,\underset{\sim}{\alpha} = \underset{\sim}{P}\,\underset{\sim}{\alpha} \tag{20}$$

where $$\underset{\sim}{P} = \underset{\sim}{T}\,\underset{\sim}{P}^* \tag{20a}$$

As shown in eq. (9), for the generation of element stiffness matrix, it is necessary to compute $\underset{\sim}{G}$ and $\underset{\sim}{H}^{-1}$. For the present nine node element the size of $\underset{\sim}{G}$ and $\underset{\sim}{H}$ matrices are 14 x 18 and 14 x 14 respectively and $\underset{\sim}{G}$ and $\underset{\sim}{H}$ matrices are evaluated using 3 x 3 point Gaussian quadrature. As far as computung time is concerned the need to evaluate $\underset{\sim}{G}$, $\underset{\sim}{H}$ and $\underset{\sim}{H}^{-1}$ makes the conventional mixed formulation less attractive than the assumed displacement formulation based on the principle of virtual work.

At this point, it is well to mention that the α_{13} and α_{14} terms in eq. (18) were chosen carefully to suppress undesirable kinematic modes. Without the α_{13} and α_{14} terms, the assumed strain field is symmetric in ξ and η. Moreover, for an element of rectangular shape, 2 x 2 point rule is sufficient enough for exact integration of $\underset{\sim}{G}$ and $\underset{\sim}{H}$. Then the resulting

stiffness matrix will be equivalent to the conventional assumed displacement model with 2 x 2 reduced integration. The equivalence between mixed formulation element and reduced or selective integration element can be proved by establishing

$$\underset{\sim}{\varepsilon} = \overline{\underset{\sim}{\varepsilon}} \tag{21}$$

at integration points. This can be done if the number of integration points is the same as the number of strain parameters or coefficients in each component of assumed strain [3,6,7]. The element without the α_{13} and α_{14} terms exhibits three kinematic modes or spurious zero strain enery modes. For a square element with sides along $x = \pm 1$ and $y = \pm 1$ lines, these spurious modes are as follows [10,11];

$$\begin{aligned} &(1)\quad u = C_1 x(1 - 3y^2) \\ &\qquad\ v = -C_1 y(1 - 3x^2) \\ &(2)\quad u = C_2(x^2 + y^2 - 3x^2y^2) \\ &(3)\quad v = C_3(x^2 + y^2 - 3x^2y^2) \end{aligned} \tag{22}$$

where C_1, C_2 and C_3 are arbitrary constants. Among these three modes, the first mode is incompatible or non-commutable as it disappears for an assembly of only two elements. The second and third modes are compatible or commutable and may persist even after assembly of elements, resulting in an unstable finite element model. The α_{13} and α_{14} terms in the assumed strain are introduced to suppress these two compatible modes. The first mode is left in the element since it is harmless. It is to be noted that the same assumed strain was used in the shell element described in reference 4 where it was found to be very effective in alleviating locking effect associated with the condition of zero inplane strain.

3. NEW FORMULATION

The proposed new formulation is also based on the Hellinger-Reissner principle with the functional given in eq. (1). However in the new formulation, the independent strain is written as

$$\underset{\sim}{\varepsilon} = \underset{\sim}{\varepsilon}_L + \underset{\sim}{\varepsilon}_H \tag{23}$$

where $\underset{\sim}{\varepsilon}_L$ is the independent strain vector with lower order polynomial terms in ξ and η. On the other hand $\underset{\sim}{\varepsilon}_H$, the higher order strain vector, contains higher order terms in ξ and η. More discussion on $\underset{\sim}{\varepsilon}_L$ and $\underset{\sim}{\varepsilon}_H$ will be given later. Inserting eq. (23) into eq. (1), the functional π_R becomes

$$\pi_R = \int (\underset{\sim}{\varepsilon}_L^T \underset{\sim}{C} \bar{\underset{\sim}{\varepsilon}} - \frac{1}{2} \underset{\sim}{\varepsilon}_L^T \underset{\sim}{C} \underset{\sim}{\varepsilon}_L) \, dA$$

$$+ \int \underset{\sim}{\varepsilon}_H^T \underset{\sim}{C} \bar{\underset{\sim}{\varepsilon}} \, dA - \int \underset{\sim}{\varepsilon}_H^T \underset{\sim}{C} \underset{\sim}{\varepsilon}_L dA$$

$$- \int \frac{1}{2} \underset{\sim}{\varepsilon}_H^T \underset{\sim}{C} \underset{\sim}{\varepsilon}_H dA - W \tag{24}$$

To help illustrate the new formulation, we will consider again nine node element. For nine node element of rectangular shape, the highest order terms in the $\bar{\underset{\sim}{\varepsilon}}$ matrix are quadratic in either ξ or η direction. Thus if the $\underset{\sim}{\varepsilon}_L$ matrix is bilinear, then the first integral can be integrated exactly using 2 x 2 point Gaussian quadrature. For $\underset{\sim}{\varepsilon}_H$, we start by assuming $\underset{\sim}{\varepsilon}_H^*$, the higher order strain vector in the local coordinate system, as

$$(\varepsilon_{xx}^*)_H = \alpha_1 f_x$$

$$(\varepsilon_{yy}^*)_H = \alpha_2 f_y \tag{25}$$

$$(\varepsilon_{xy}^*)_H = 0$$

Or in matrix form,

$$\underset{\sim}{\varepsilon}_H^* = \underset{\sim}{\overline{P}}^* \underset{\sim}{\alpha} \tag{26}$$

where

$$\underset{\sim}{\overline{P}}^* = \begin{bmatrix} f_x & 0 \\ 0 & f_y \\ 0 & 0 \end{bmatrix} \tag{26a}$$

$$\underset{\sim}{\alpha} = \begin{Bmatrix} \alpha_1 \\ \alpha_2 \end{Bmatrix} \tag{26b}$$

Note that $\underset{\sim}{\varepsilon}_H^*$ contains the higher order α_{13} and α_{14} terms of the conventional formulation given in the previous section. Using the strain transformation matrix $\underset{\sim}{T}$, the $\underset{\sim}{\varepsilon}_H$ vector in the global coordinate system is expressed as

$$\underset{\sim}{\varepsilon}_H = \underset{\sim}{T}\, \underset{\sim}{\varepsilon}_H^* = \underset{\sim}{T}\, \underset{\sim}{\overline{P}}^* \alpha = \underset{\sim}{\overline{P}}\, \underset{\sim}{\alpha} \tag{27}$$

where $$\underset{\sim}{\overline{P}} = \underset{\sim}{T}\, \underset{\sim}{\overline{P}}^* \tag{27a}$$

Of course, for rectangular element, $\underset{\sim}{\overline{P}}$ is equal to $\underset{\sim}{\overline{P}}^*$. However, for an element of arbitrary shape, strain transformation in eq. (27) is used. Again, for rectangular element, the third integrals in eq. (24) require 2 x 2 point rule. On the other hand the second and fourth integrals require 3 x 3 point rule. For an element with arbitrary shape the argument regarding the number of integration points for exact integration does not hold. However even in this case the same integration rules will be adopted.

In addition, for the first and third integrals, we may write $\underset{\sim}{\varepsilon}_L$ as

$$\underset{\sim}{\varepsilon}_L = \sum_{i=1}^{4} \bar{N}_i(\xi,\eta)\bar{\underset{\sim}{\varepsilon}}_i \tag{28}$$

where $\bar{N}_i$ are bilinear shape function such that $\bar{N}_i = 1$ at the point i of the 2 x 2 point integration and zero otherwise, and $\bar{\underset{\sim}{\varepsilon}}_i$ is the strain $\bar{\underset{\sim}{\varepsilon}}$ evaluated at integration point i. In another word, we can set

$$\underset{\sim}{\varepsilon}_L = \bar{\underset{\sim}{\varepsilon}} \tag{29}$$

at 2 x 2 integration points.

Introducing eq. (29) to eq. (24),

$$\pi_R = \int_L \frac{1}{2}\underset{\sim}{\varepsilon}_L^T \underset{\sim}{C}\, \underset{\sim}{\varepsilon}_L dA + \int_H \underset{\sim}{\varepsilon}_H^T \underset{\sim}{C}\, \bar{\underset{\sim}{\varepsilon}} dA - \int_L \underset{\sim}{\varepsilon}_H^T \underset{\sim}{C}\, \underset{\sim}{\varepsilon}_L dA$$

$$- \int_H \frac{1}{2}\underset{\sim}{\varepsilon}_H^T \underset{\sim}{C}\, \underset{\sim}{\varepsilon}_H dA - W \tag{30}$$

In eq. (30), letters L and H under the integral signs indicate lower order integration (2 x 2 point rule) and higher order integration (3 x 3 point rule) respectively. Introducing eqs. (3) and (26) into eq. (30) and noting eq. (29), π_R can be written as

$$\pi_R = \sum_e \left(\frac{1}{2}\underset{\sim}{q}_e^T \underset{\sim}{K}_L \underset{\sim}{q}_e + \underset{\sim}{\alpha}^T \bar{\underset{\sim}{G}}\, \underset{\sim}{q}_e - \frac{1}{2}\underset{\sim}{\alpha}^T \bar{\underset{\sim}{H}}\, \underset{\sim}{\alpha} - \underset{\sim}{q}_e^T \underset{\sim}{Q}_e\right) \tag{31}$$

where

$$\underset{\sim}{K}_L = \int_L \underset{\sim}{B}^T \underset{\sim}{C}\, \underset{\sim}{B} \left| \underset{\sim}{J} \right| d\xi\, d\eta \tag{31a}$$

$$\bar{\underset{\sim}{G}} = \underset{\sim}{G}_H - \underset{\sim}{G}_L \tag{31b}$$

$$\underset{\sim}{G}_H = \int_H \overline{\underset{\sim}{P}}^T \underset{\sim}{C}\ \underset{\sim}{B} \left| \underset{\sim}{J} \right| d\xi\ d\eta \tag{31c}$$

$$\underset{\sim}{G}_L = \int_L \overline{\underset{\sim}{P}}^T \underset{\sim}{C}\ \underset{\sim}{B} \left| \underset{\sim}{J} \right| d\xi\ d\eta \tag{31d}$$

$$\overline{\underset{\sim}{H}} = \int_H \overline{\underset{\sim}{P}}^T \underset{\sim}{C}\ \overline{\underset{\sim}{P}} \left| \underset{\sim}{J} \right| d\xi\ d\eta \tag{39e}$$

and $\left| \underset{\sim}{J} \right|$ is the determinant of Jacobian matrix $\underset{\sim}{J}$. Note that, although the same symbol $\underset{\sim}{B}$ appears in $\underset{\sim}{K}_L$, $\underset{\sim}{G}_H$ and $\underset{\sim}{G}_L$, $\underset{\sim}{B}$ in $\underset{\sim}{G}_H$ is evaluated at 3 x 3 Gaussian integration points while $\underset{\sim}{B}$ in $\underset{\sim}{K}_L$ and $\underset{\sim}{G}_L$ is evaluated at 2 x 2 Gaussian integration points. However to save computing time, the $\underset{\sim}{B}$ matrix at 2 x 2 integration points can be interpolated from the $\underset{\sim}{B}$ matrix evaluated at 3 x 3 integration points. That is, we evaluate $\underset{\sim}{B}$ at 2 x 2 points from the following expression:

$$\underset{\sim}{B} = \sum_{i=1}^{9} \tilde{N}_i(\xi,\eta)\underset{\sim}{B}_i \tag{32}$$

where $\underset{\sim}{B}_i$ is the $\underset{\sim}{B}$ matrix at the integration point i and $\tilde{N}_i$ is the shape function such that $N_i = 1$ at point i of the 3 x 3 integration points and zero at other points. In addition the determinant $\left| \underset{\sim}{J} \right|$ at 2 x 2 integration points is also interpolated from $\left| \underset{\sim}{J} \right|$ at 3 x 3 integration points.

Taking $\delta\pi_R$ with respect to $\underset{\sim}{\alpha}$ of each element

$$\overline{\underset{\sim}{H}}\ \underset{\sim}{\alpha} - \overline{\underset{\sim}{G}}\underset{\sim}{q}_e = 0 \tag{33}$$

or solving for α

$$\underset{\sim}{\alpha} = \overline{\underset{\sim}{H}}^{-1}\ \overline{\underset{\sim}{G}}\ \underset{\sim}{q}_e \tag{34}$$

for each element.

Substituting eq. (34) into eq. (31),

$$\pi_R = \sum(\frac{1}{2} \underset{\sim}{q}_e^T \underset{\sim}{K}_e \underset{\sim}{q}_e - \underset{\sim}{q}_e^T \underset{\sim}{Q}_e) \tag{35}$$

where

$$\underset{\sim}{K}_e = \underset{\sim}{K}_L + \overline{\underset{\sim}{G}}^T \overline{\underset{\sim}{H}}^{-1} \overline{\underset{\sim}{G}} \tag{36}$$

is the element stiffness matrix. Assembling over all elements

$$\pi_R = \frac{1}{2}\underset{\sim}{q}^T \underset{\sim}{K} \underset{\sim}{q} - \underset{\sim}{q}^T \underset{\sim}{Q} \tag{37}$$

where $\underset{\sim}{K}$ is the global stiffness matrix corresponding to the global displacement vector $\underset{\sim}{q}$ and $\underset{\sim}{Q}$ is the global load vector. Taking $\delta\pi_R = 0$ with respect to $\underset{\sim}{q}$ results in

$$\underset{\sim}{K}\, \underset{\sim}{q} = \underset{\sim}{Q} \tag{38}$$

which can be solved for $\underset{\sim}{q}$. With $\underset{\sim}{q}$ and thus $\underset{\sim}{q}_e$ known strain $\underset{\sim}{\varepsilon}$ is determined from eqs. (23), (27), (28) and (34) as follows:

$$\underset{\sim}{\varepsilon} = \underset{\sim}{\varepsilon}_L + \underset{\sim}{\varepsilon}_H = \underset{\sim}{\varepsilon}_L + \overline{\underset{\sim}{P}}\underset{\sim}{\alpha}$$

$$= \sum_{i=1}^{4} \overline{\underset{\sim}{N}}_i \underset{\sim}{B}_i \underset{\sim}{q}_e + \overline{\underset{\sim}{P}}\, \overline{\underset{\sim}{H}}^{-1} \overline{\underset{\sim}{G}} \underset{\sim}{q}_e \tag{39}$$

Then stress $\underset{\sim}{\sigma}$ is determined by eq. (13).

It should be pointed out that the element stiffness matrix in eq. (36) has two components, $\underset{\sim}{K}_L$ and $\overline{\underset{\sim}{G}}^T \overline{\underset{\sim}{H}}^{-1} \overline{\underset{\sim}{G}}$. For an element of rectangular shape the $\underset{\sim}{K}_L$ matrix is the same as the stiffness matrix of the conventional assumed displacement model with 2 x 2 reduced integration. Again the equivalence is established through eq. (29). Then the $\underset{\sim}{K}_L$ matrix has the same three kinematic

modes given in eq. (22). With the addition of $\bar{\underset{\sim}{G}}^T \bar{\underset{\sim}{H}}^{-1} \bar{\underset{\sim}{G}}$ matrix, the compatible kinematic modes are suppressed, leaving only the incompatible mode. Therefore, as far as kinematic modes are concerned, both the conventional formulation and the new formulation result in the same incompatible mode. However element stiffness matrix from the new formulation is not exactly the same as that from the conventional formulation. The size of $\bar{\underset{\sim}{G}}$ and $\bar{\underset{\sim}{H}}$ matrices in the new formulation are 2 x 18 and 2 x 2 respectively. Therefore, computation of the $\bar{\underset{\sim}{G}}^T \bar{\underset{\sim}{H}}^{-1} \bar{\underset{\sim}{G}}$ matrix in the new formulation can be carried out without much effort. Recall that in the conventional formulation, the sizes of $\underset{\sim}{G}$ and $\underset{\sim}{H}$ matrices are 14 x 18 and 14 x 14 respectively. Note also that the present element passes the patch test.

4. COMPARATIVE NUMERICAL TEST

(a) Comparison of Computing Time

In order to evaluate computing efficiency of the new formulation, a test was run in which stiffness matrix of single nine node element was computed 40 times consecutively. Table 1 shows relative computing time for different element types. Clearly the new mixed formulation element (NM) requires much less computing time than the conventional mixed formulation element (CM). Surprisingly the new mixed formulation takes less computing time than the conventional assumed displacement element with 3 x 3 point rule (DISP3). Of course the assumed displacement element with 2 x 2 point rule (DISP2) takes the least time. However, as mentioned before, this element has compatible kinematic modes and thus cannot be used in general stress analysis.

(b) A Panel under a Horizontal Point Load

Figure 2 shows a rectangular panel subjected to a horizontal point load P.

The panel is modeled by 2 x 12 mesh as shown in the figure. Two boundary conditions are considered. In case 1, the left end is completely fixed. In case 2, the vertical displacements of the first, second, fourth and fifth nodes along the left end are left unconstrained. The first case has been used in references 13 and 14 to demonstrate the undesirable effect of spurious kinematic modes on numerical solution. The pertinent data are as follows;

length L = 12m

depth b = 2m

Poissons ratio $\nu = 0.2$

$P/AE = \frac{1}{480}$

where E is the Young's modulus and A is the cross-sectional area. Table 2 lists the nondimensional horizontal displacement calculated at the load point for the NM, CM, DISP2 and DISP3 elements. Numerical solutions are nondimensionalized by dividing the computed values by the tip displacement PL/AE of a panel under total load P distributed uniformly over the cross-sectional area. The solution for the DISP2 element is very large compared with those obtained by the other three element types, especially in case 2. This is due to the spurious compatible kinematic modes in the DISP2 element triggered by the point load. The NM, CM elements are free of compatible kinematic modes and the DISP3 element has no kinematic mode. Therefore they provide stable solutions.

(c) A Cantilever Beam

A cantilever beam subjected to a tip load P is used to evaluate the performance of the present new element as compared to the conventional mixed formulation element and the assumed displacement model element. Note again that the same problem has been used as a numerical example in reference 13. As illustrated in fig. 3, the cantilever beam is modelled by three different

finite element meshes. Two different length to depth ratios of 10 and 20 are considered. Table 3 lists computed vertical displacement of point A in fig. 3 and stress σ_{xx} evaluated at point B. The point B is one of the Gaussian points in the 2 x 2 integration rule. Numerical solutions were normalized by the following solutions obtained from the Bernoulli-Euler beam theory:

$$v_A = PL^3/3EI$$
$$(\sigma_{xx})_B = M\, y_B/I \tag{41}$$

where

I = sectional area moment of inertia

M = bending moment

y_B = y coordinate of point B

Numerical results in Table 3 indicates that NM, CM and DISP2 elements perform much better than the DISP3 element especially for meshes with non-rectangular elements. For this particular example, the NM element seems to be better than the CM element. It is interesting to note that, for the present problem under vertical tip load, the spurious kinematic modes of the DISP2 elements remain untriggered as indicated by the stable solution. This is in sharp contrast to the previous example under horzontal point load.

5. FOUR NODE ELEMENT

For four node element, a finite element model based on the conventional mixed formulation may be developed by assuming independent strain vector $\underset{\sim}{\varepsilon}^*$ defined with respect to the local coordinate system as follows:

$$\varepsilon^*_{xx} = \alpha_1 + \alpha_4 g_x$$
$$\varepsilon^*_{yy} = \alpha_2 + \alpha_5 g_y \tag{42}$$
$$\varepsilon^*_{xy} = \alpha_3$$

In eq. (42), $g_x = \eta$ and $g_y = \xi$ for $\underset{\sim}{a}_1$ defined as in eq. (16). For $\underset{\sim}{a}_1$ defined as in eq. (17), g_x and g_y are chosen as $g_x = \xi$ and $g_y = \eta$. Again strain $\underset{\sim}{\varepsilon}$ in the global coordinate system is obtained from $\underset{\sim}{\varepsilon}^*$ through strain transformation as shown in eq. (20). As for numerical integration, the $\underset{\sim}{G}$ and $\underset{\sim}{H}$ matrices in the conventional formulation are evaluated by 2 x 2 point rule. For a finite element model based on the new formulation, the higher order strain $\underset{\sim}{\varepsilon}_H$ in the local coordinate system is assumed as

$$(\varepsilon^*_{xx})_H = \alpha_1 g_x$$

$$(\varepsilon^*_{yy})_H = \alpha_2 g_y \qquad (42)$$

$$(\varepsilon^*_{xy})_H = 0$$

Again $\underset{\sim}{\varepsilon}_H$ in the global coordinate system is determined from $\underset{\sim}{\varepsilon}^*_H$ through strain transformation. As for numerical integration, the $\underset{\sim}{K}_L$ and $\underset{\sim}{G}_L$ matrices are evaluated by one point integration rule whereas 2 x 2 point rule is used for integration of $\underset{\sim}{G}_H$ and $\overline{\underset{\sim}{H}}$ in the new formulation. Of course in computing $\underset{\sim}{K}_L$ and $\underset{\sim}{G}_L$, $\underset{\sim}{B}$ matrices and $|\underset{\sim}{J}|$ at the integration point can be interpolated from $\underset{\sim}{B}$ matrix and $|\underset{\sim}{J}|$ evaluated at 2 x 2 initegration points following the similar procedure used for the nine node element. For an element of rectangular geometry, the $\underset{\sim}{K}_L$ matrix is the same as the stiffness matrix of four node assumed displacement element based on the principle of virtual work with one point integration. The $\underset{\sim}{K}_L$ matrix has two compatible spurious kinematic modes. However addition of the $\overline{\underset{\sim}{G}}^T \overline{\underset{\sim}{H}}^{-1} \overline{\underset{\sim}{G}}$ matrix as shown in eq. (36) suppresses these kinematic modes and thus element stiffness matrix $\underset{\sim}{K}_e$ is stable and has correct rank. For an element of rectangular shape, the new formulation element is equivalent to the element based on the conventional formulation. Furthermore, it is found that for an element with square geometry, the present element is equal to the Belytschko's four node element with a properly chosen stabilization

matrix [12]. The element stiffness matrix of Belytschko's four node element described in reference 12 may be expressed as

$$\underset{\sim}{K}_e = \underset{\sim}{K}_L + \underset{\sim}{K}_s \tag{43}$$

where

$$\underset{\sim}{K}_s = \frac{Et}{1-\nu^2} \begin{bmatrix} C_1 \chi_1^T \chi_1 & 0 \\ 0 & C_2 \chi_2^T \chi_2 \end{bmatrix} \tag{44}$$

is the stabilization matrix introduced to suppress kinematic modes in $\underset{\sim}{K}_L$. The constants C_1 and C_2 are control parameters and the expression for χ_1 and χ_2 are given in reference 12. If we set $C_1 = C_2 = 1/12$, then for a square element, the resulting stiffness matrix is exactly the same as that of the present four node element.

6. DISCUSSION AND CONCLUSION

Numerical test with nine node element indicates that the proposed new formulation needs less than half of the computing time required for the conventional mixed formulation to generate element stiffness matrix. Also for nine node element the computing time for new element is slightly less than that required for the conventional assumed displacement model with 3 x 3 point integration. The nine node element based on the new formulation is not exactly the same as that based on the conventional mixed formulation. However they are very close to each other. For four node element, the

conventional and new formulation result in the same stiffness matrix for rectangular element geometry. Also equivalence to Belytschko's four node element with properly adjusted stabilization control parameters has been observed. It is to be noted that the $\underset{\sim}{\overline{G}}^T \underset{\sim}{\overline{H}}^{-1} \underset{\sim}{\overline{G}}$ matrix in eq. (36) associated with higher order assumed independent strain plays the role of stabilization matrix. As such the present new approach can be viewed as an alternative way of introducing stabilization matrix into the finite element formulation. The present formulation can be easily extended to two and three dimensional problems, as well as thin plate and shell problems. In fact a new approach applied to shell element formulation will be the subject of a forthcoming paper. Also extension to nonlinear problems seems to be straightforward.

ACKNOWLEDGEMENT

The present work was supported by the Office of Naval Research (N00014-84-K-0385).

REFERENCES

1. T.H.H. Pian, "Reflections and remarks on hybrid and mixed finite element methods," Hybrid and Mixed Finite Element Methods, Edited by S.N. Atluri, R.H. Gallagher and O.C. Zienkiewicz, Wiley, (1983).
2. T.H.H. Pian, "Derivation of element stiffness matrices by assumed stress distribution," AIAA J., 2, 1333-1334, (1964).
3. S.W. Lee and T.H.H. Pian, "Improvement of plate and shell finite element by mixed formulations," AIAA J. 16, 29-34, (1978).
4. S.W. Lee, S.C. Wong and J.J. Rhiu, "Study of a nine node mixed formulation finite element for thin plates and shells", Computers and Structures, 21, 1325-1334 (1985).
5. T.H.H. Pian and S.W. Lee, "Notes on finite elements for nearly incompressible materials," AIAA J., 14, 824-826, (1976).
6. S.W. Lee, "Finite element methods for reduction of constraints and creep analysis," Ph.D. dissert., Dept. of Aero. and Astro., MIT, Feb. 1978.
7. D.S. Malkus and T.J.R. Hughes, "Mixed finite element methods - reduced and selective integration techniques: a unification of concepts," Comp. Meths. Appl. Mech. Eng. 15, 63-81, (1978).
8. A.K. Noor and J.M. Peters, "Mixed models and reduced/selective integration displacement models for nonlinear analysis of curved beams," Int. J. Num. Meth. Eng. 17, 615-631, (1981).
9. L.R. Herrmann, "A bending analysis of plates", Proc. Conf. Matrix Method in Struc. Mech., AFFDL-TR-66-80, 577-604 (1966).

10. H. Parisch, "A critical survey of the 9-node degenerated shell element with special emphasis on thin shell application and reduced integration," Comp. Meths. Appl. Mech. Eng. 20, 323-350, (1979).

11. S.C. Wong, "A nine node assumed strain finite element model for analysis of thin shell structures," Ph.D. dissert., Dept of Aerospace Eng., Univ. of Maryland, (1985).

12. D.P. Flanagan and T. Belytschko, "A uniform strain hexahedron and quadrilateral with orthogonal hourglass control," Int. J. Numer. Meth. Eng. 17, 696-706 (1981).

13. R.D. Cook and Z.H. Feng, "Control of spurious modes in the nine-node quadrilateral element," Int. J. Numer. Meth. Eng., 18, 1576-1580 (1982).

14. N. Bicanic and E. Hinton, "Spurious modes in two-dimensional isoparametric elements," Int. J. Numer. Meth. Eng, 14, 1545-1557 (1979).

Table 1. Relative Computing Time to Generate the Stiffness Matrix of Nine Node Element

Element Type	Relative Time
DISP3	1.0
DISP2	0.53
CM	1.95
NM	0.89

Table 2. Nondimensional Horizontal Displacement at the Load Point of a Cantilever Panel.

Element Type	NM	CM	DISP3	DISP2
Case 1	1.3087	1.2456	1.2116	147.62
Case 2	1.3096	1.2466	1.2126	7.4928×10^{15}

Table 3. Nondimensional Vertical Deflection and Flexural Stress for a Cantilever Beam

Mesh Type		1		2		3	
L/b	Type	$\bar{v}_A$	$\bar{\sigma}_B$	$\bar{v}_A$	$\bar{\sigma}_B$	$\bar{v}_A$	$\bar{\sigma}_B$
10	NM	.9950	1.0223	1.0141	1.0848	.9875	.9805
	CM	.9900	1.0000	.9748	.9140	.9603	.9228
	DISP3	.9541	1.1407	.7913	.6957	.7370	.7745
	DISP2	1.0058	1.0000	1.1085	1.1253	.9549	.9584
20	NM	.9902	1.0223	.9905	1.0045	.9833	.9933
	CM	.9850	1.0000	.9672	.9003	.9556	.9228
	DISP3	.9362	1.1931	.7584	.6833	.4406	.4871
	DISP2	1.0014	1.0000	1.1036	1.1253	.9506	.9584

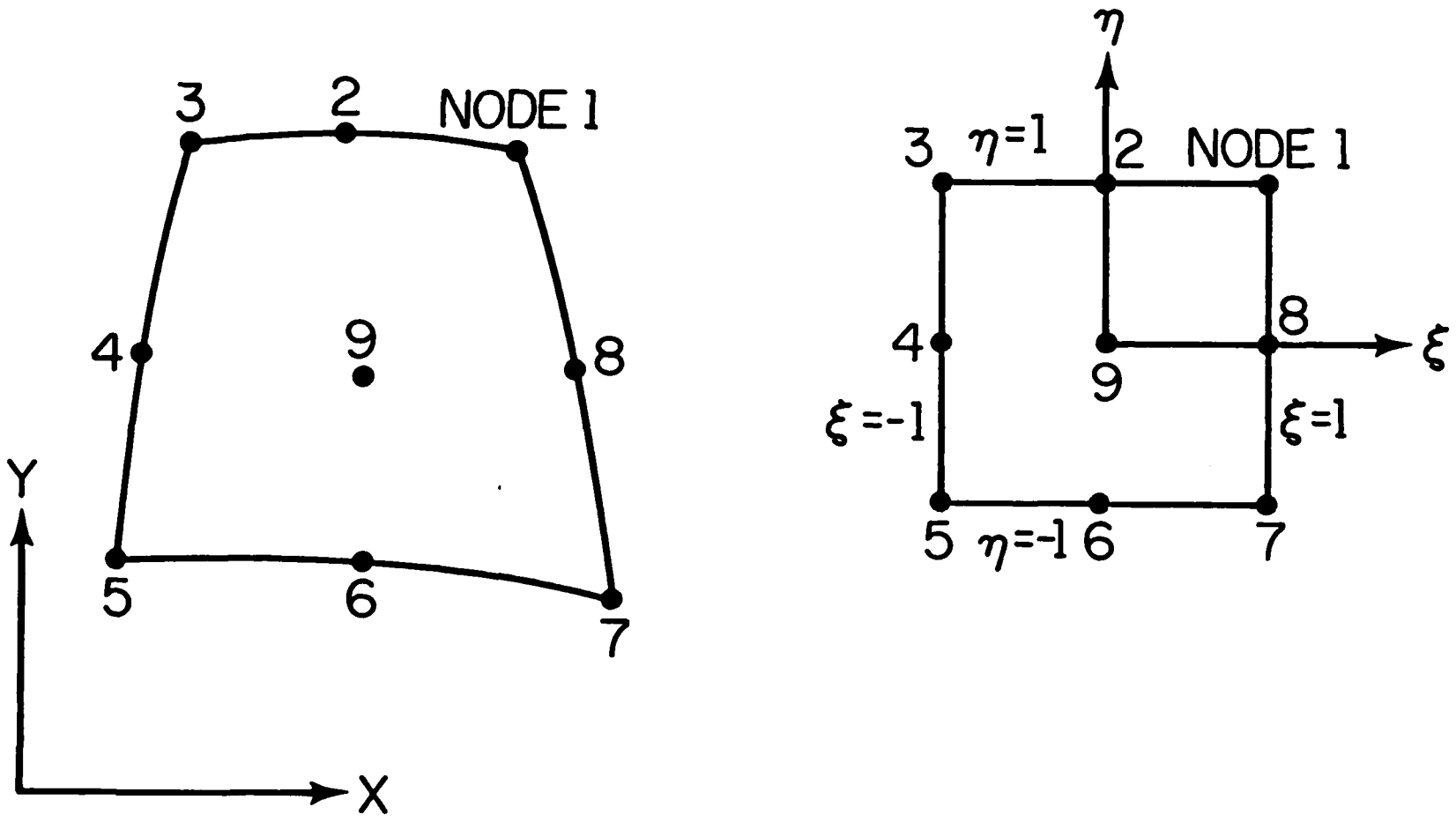

Fig. 1 Nine Node Element

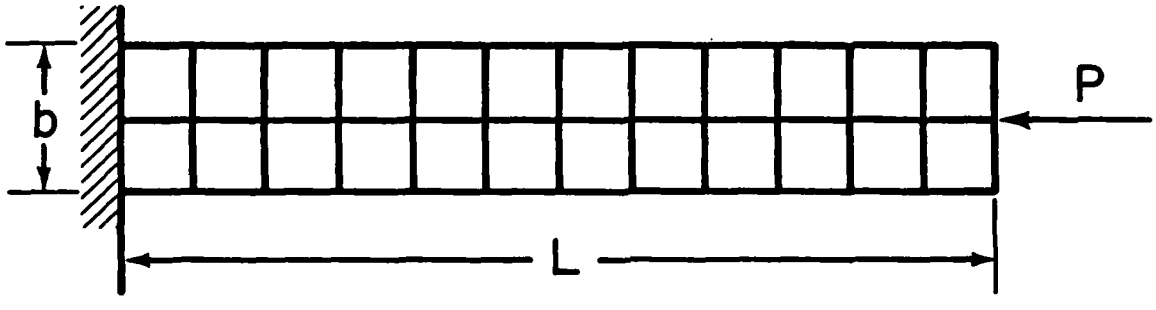

Fig. 2 A Panel under a Horizontal Point Load

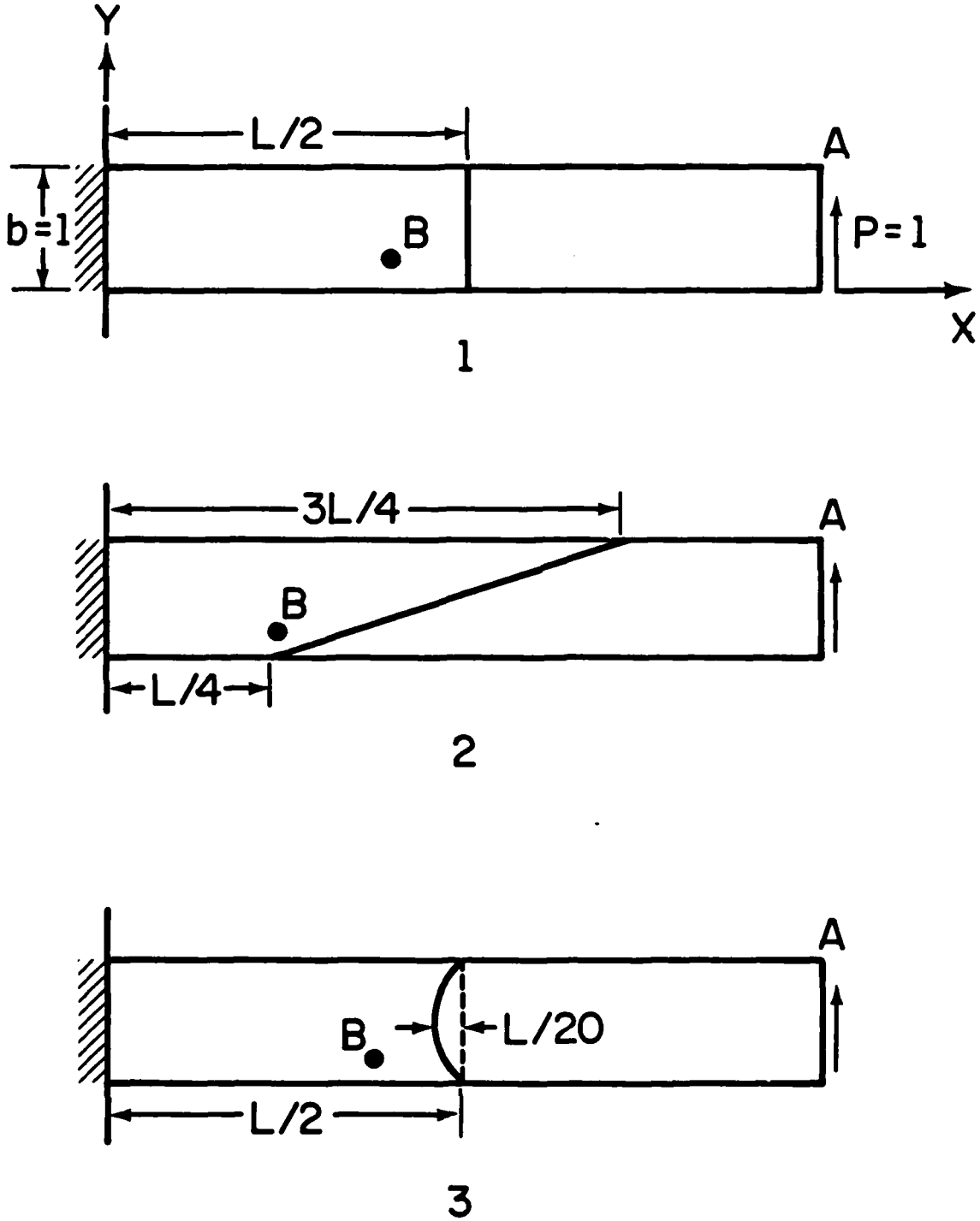

Fig. 3 Finite Element Meshes for a Cantilever Beam under Tip Load

END

FILMED

6-86

DTIC